Journal of Materials Chemistry B

ROYAL SOCIETY OF CHEMISTRY

PAPER

View Article Online
View Journal | View Issue

Check for updates

Cite this: J. Mater. Chem. B, 2024, 12, 9760

Extracellular vesicles containing fullerene derivatives prepared by an exchange reaction for photodynamic therapy†

Nanami Kono,‡[a] Riku Kawasaki, ‡*[a] Ayano Oshige,[a] Kotaro Nishimura,[a] Keita Yamana,[a] Dilimulati Yimiti,[b] Shigeru Miyaki,[b] Nobuo Adachi,[b] Naoki Takabayashi,[c] Takeshi Nagasaki[c] and Atsushi Ikeda *[a]

Received 28th February 2024,
Accepted 26th August 2024

DOI: 10.1039/d4tb00416g

rsc.li/materials-b

Extracellular vesicles (EVs) have excellent biocompatibility and long retention times in the circulation and have consequently been expected to be useful as drug-delivery systems. However, their applications have been limited because of the inability to introduce hydrophobic compounds to EVs without the use of harmful organic solvents. Herein, we developed an organic-solvent-free drug-loading technique based on the host exchange reaction. We demonstrated that the exchange reaction enabled quantitative loading of EVs with highly concentrated (0.1 mM) hydrophobic fullerene derivatives. Fullerene derivative–loaded EVs (EVs/C_{60}) could eliminate cancer cell lines more efficiently than fullerene derivative-loaded liposomes (Lip/C_{60}). Moreover, the photodynamic activity of EVs/C_{60} was fivefold higher than that of the clinically available photosensitizer photofrin. EVs/C_{60} could efficiently suppress tumor growth in tumor-xenograft model mice.

Published on 31 August 2024. Downloaded on 2/13/2026 2:46:06 PM.

Introduction

With low immunogenicity and targeting properties, extracellular vesicles (EVs)[1,2] are expected to be used as bio-based drug-delivery systems. Moreover, EVs can provide internal spaces that can entrap hydrophilic and hydrophobic pharmaceuticals in the same manner as liposomes. EVs derived from plants are also emerging as drug-delivery platforms.[3,4] Large masses of EVs can be derived from plants and could potentially solve some of the problems encountered in the formulation of EV-based pharmaceuticals in clinical applications. To expand their applicability as drug-delivery platforms, the development of drug-loading methods is indispensable. Although a large proportion of clinically available drugs are hydrophobic, the technology to encapsulate hydrophobic compounds for EVs remains challenging.[4,5] Existing encapsulation methods for EVs include physical techniques such as sonication, electroporation, extrusion, and agitation; however, concerns remain that external stimuli can disrupt the structure of EVs.[4] In loading hydrophobic compounds to EVs, these compounds have to be initially dissolved in organic solvents such as DMSO and ethanol that can mix with water arbitrarily and the resulting solution should be injected into the EV dispersion. However, the molecules that can dissolve in these organic solvents are limited and they can easily develop undesirable aggregates after injection into aqueous media. Moreover, organic solvents can induce the denature of membrane proteins in EVs, disorganize the membrane structure of EVs, and have harmful effects on biologics.[6,7] Consequently, the development of organic-solvent free techniques to introduce hydrophobic compounds to EVs is required to expand their applicability as drug carriers.[4]

Our group has established the loading methodology of hydrophobic compounds for liposomes based on host exchange, and the exchange reaction can efficiently encapsulate compounds such as fullerenes and porphyrins into lipid bilayersquantitatively at high concentration without using organic solvents.[8–10] Moreover, the encapsulated molecules maintain their pharmacological activities, such as photo-reactivity, photodynamic activity, and anticancer effects.[8] These advantages in the exchange reaction encouraged us to employ current methods to introduce fullerene, a hydrophobic compound, into EVs and to demonstrate the photodynamic activity of fullerene derivatives loaded into EVs for photo-triggered cancer treatment.

[a] Program of Applied Chemistry, Graduate School of Advanced Science and Engineering, Hiroshima University, 1-4-1 Kagamiyama, Higashi Hiroshima, 739-8527, Japan. E-mail: riku0528@hiroshima-u.ac.jp, aikeda@hiroshima-u.ac.jp
[b] Department of Orthopaedic Surgery, Graduate School of Biomedical and Health Sciences, Hiroshima University, 1-2-3 Kasumi Minami-ku, Hiroshima, 734–8551, Japan
[c] Department of Applied Chemistry and Bioengineering, Graduate School of Osaka Metropolitan University, 3-3-138 Sugimoto, Sumiyoshi-ku, Osaka, 558-8585, Japan

† Electronic supplementary information (ESI) available: Details of the experimental procedure and analytical data. See DOI: https://doi.org/10.1039/d4tb00416g

‡ These authors contributed equally to this work.

This journal is © The Royal Society of Chemistry 2024

Published on 31 August 2024. Downloaded on 2/13/2026 2:46:06 PM.

Photodynamic therapy (PDT)[11,12] is a photochemistry-based cancer treatment that is minimally invasive because the light can be controlled with spatiotemporal high resolution. Cancer cell destruction in PDT is achieved by cytotoxic reactive oxygen species (ROS), including singlet oxygen ($^1O_2$), generated by photosensitizers[13] *via* laser irradiation. Since the lifetime of these ROS is short,[14] the deliverability of photosensitizers to cancer cells is a key technology. Fullerenes,[9,15] porphyrins,[10,16] and phthalocyanines[17] have been studied as photosensitizers for biologics because of their excellent conversion rate and absorbability in red light regions that can travel deeper from the tissue surface; however, their biomedical use is limited because of the hydrophobicity of the compounds, instability in aqueous media, and poor tumor-targeting properties. To address these issues, modification of hydrophilic moieties such as sulfonyl groups and ethylene glycol units to the compounds has been employed, although these conjugations can easily reduce the intended photodynamic activity. However, encapsulation of photosensitizers into drug-delivery systems is a powerful means of enhancing the water dispersibility and cancer-targeting properties of photosensitizers. Therefore, EVs are considered attractive platforms to establish photosensitizers with high anti-tumor efficacy.

Herein, we developed an organic solvent free drug-loading method for EVs *via* an exchange reaction and demonstrated the photodynamic activity of fullerene-loaded lemon-derived EVs for cancer treatment *in vitro* and *in vivo* (Fig. 1).

Results and discussion

Preparation of EVs incorporating fullerenes *via* a host molecule exchange reaction

Plant-derived EVs are easily extractable and exhibit several benefits for human health for treating cancer and inflammation because they contain plant-derived biologically active molecules,[3,4] such as polyphenols, flavonoids, and ceramides. Therefore, plant-derived EVs have been expected to be candidate delivery platforms for pharmaceuticals. Herein, we focused on lemon, which is one of the major fruits produced in Hiroshima, Japan. EVs were isolated by fractional centrifugation of lemon juice from squeezed lemons (purchased from a local supermarket) as reported by other groups.[18] The size distribution of the EVs was confirmed by nano-tracking analysis (NTA), and the morphology of the EVs was observed by transmission electron microscopy (TEM). The NTA-derived average particle size was approximately 180 nm (Fig. 2a, black line) while spherical structures with a diameter of 150–200 nm were observed *via* transmission electron microscopy (TEM) (Fig. 2b). A total of 2.4×10^{12} particles were obtained from 100 g of lemons used for isolation of EVs and contained 0.5 mg mL^{-1} protein and 7.5 mg dL^{-1} lipid. Thus, the current method enabled the preparation of large amounts of EVs, and such scalability is appealing for formulation compared with other EV sources such as cultured cell lines. In this study, we employed liposomes as a control, which were prepared using 1,2-dimyristoyl-*sn*-glycero-3-phosphocholine using the freeze–thaw method. After size extrusion, the size distribution of liposomes was evaluated *via* dynamic light scattering (DLS), and their size was determined to be approximately 100 nm (polydispersity index, 0.09; Table 1).

Since a highly concentrated fullerene derivative solution is required to introduce fullerene derivatives into EVs, we initially prepared a fullerene–γ-cyclodextrin complex (C_{60}·γ-CD) (C_{60}-**1**, 2.7 mg; 3 μmol: C_{60}-**2**, 2.4 mg; 3 μmol: γ-CD, 15.6 mg; 12 μmol) *via* high speed vibration milling (HSVM) as previously reported.[8,9,19] The complexation of fullerene derivatives with γ-CD (C_{60}-**1**·γ-CD and C_{60}-**2**·γ-CD) was confirmed *via* ^{1}H-nuclear magnetic resonance (NMR) spectroscopy (Fig. 2c top panel and Fig. S1 top panel, ESI†). For C_{60}-**1**, methyl groups in C_{60}-**1** were found at 2.2 ppm. Similarly, a representative peak at 2.1 ppm from the methyl group in C_{60}-**2** appeared after complexation. These results indicate that the fullerene derivatives were successfully dissolved in water. We evaluated the concentration of fullerene derivatives in each solution by measuring UV-Vis absorption spectra (Fig. 2d and Fig. S2, ESI†), and the concentrations of C_{60}-**1**·γ-CD and C_{60}-**2**·γ-CD were determined to be 0.7 and 0.61 mM, respectively (C_{60}-**1**, $\varepsilon_{322} = 4.31 \times 10^4$ cm^{-1} mol^{-1} dm^3; C_{60}-**2**; $\varepsilon_{324} = 4.02 \times 10^4$ cm^{-1} mol^{-1} dm^3). As previously reported,[9,19] we obtained highly concentrated fullerene solutions for the exchange reaction.

We next conducted an exchange reaction with EVs using the complex of fullerene derivatives with γ-CD. The exchange reaction can proceed by mixing EVs and C_{60}·γ-CD complex (C_{60}, 0.20 mM; EVs, 0.25 mg mL^{-1}) in aqueous media at 40 °C. The progress of the exchange reaction was traced by evaluating ^{1}H-NMR and UV-vis spectra at each time point (0, 3, and 7 days). When the fullerenes were translocated from cyclodextrin complex to EVs, their diffusion got slower, resulting in the peaks from fullerenes in NMR get broadened and disappeared. The peaks assignable to C_{60}-**2**·γ-CD at 2.05 ppm gradually broadened with time (Fig. 2c middle and bottom panel), as we previously reported in the case of the liposomal

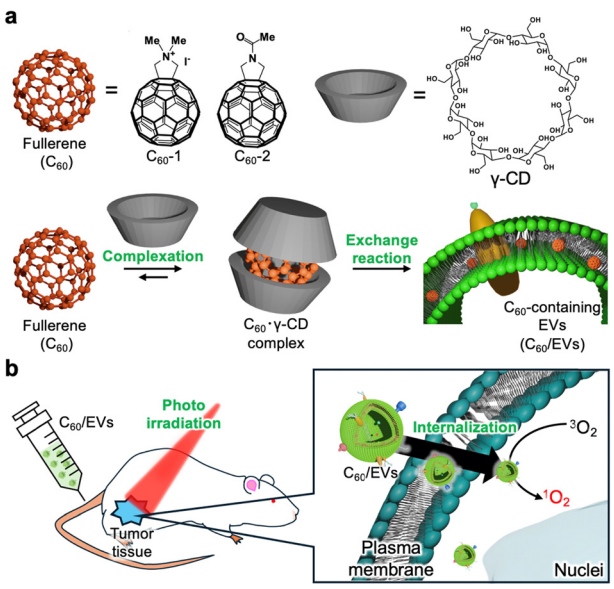

Fig. 1 Schematic of the preparation of C_{60} derivative–containing EVs and their application as photosensitizers. (a) Chemical structure and schematic of the integration of fullerenes within EVs *via* an exchange reaction. (b) Application of C_{60}/EVs as photosensitizers for cancer therapy.

Published on 31 August 2024. Downloaded on 2/13/2026 2:46:06 PM.

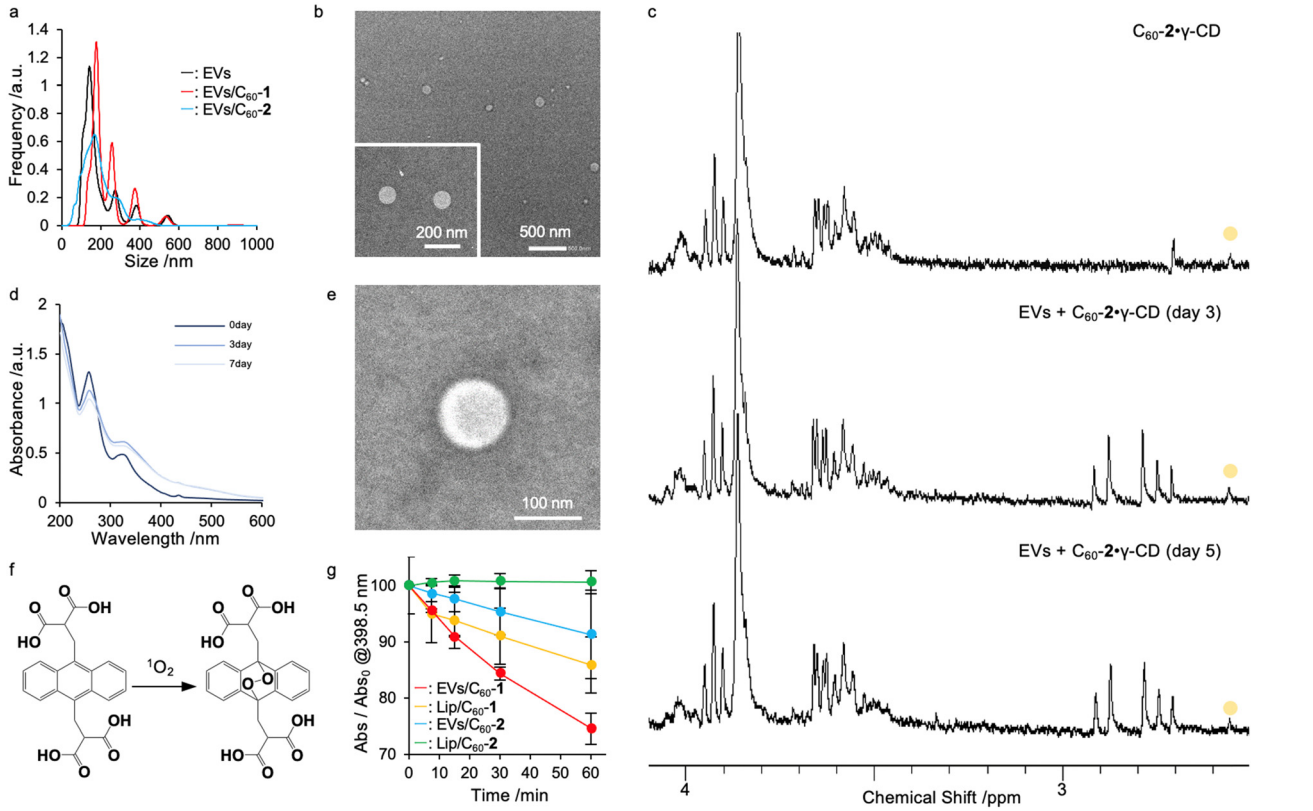

Fig. 2 Characterization of fullerene C_{60} derivative–loaded EVs (a) Size distribution of EVs and C_{60} derivative–loaded EVs (black, EVs; red, EVs/C_{60}-**1**; blue, EVs/C_{60}-**2**). (b) Representative morphology of EVs. Inset represents a highly magnified image of EVs. Samples cast on a grid were stained with 0.1% phosphotungstic acid and were then observed *via* TEM (acceleration voltage, 80 kV). (c) Introduction of C_{60} derivatives into the membrane of EVs *via* an exchange reaction. ^{1}H-NMR spectra of C_{60}-**2** complexed with γ-CDx in D_2O (top panel). ^{1}H-NMR spectra of the mixture of C_{60}-**2** complexed with γ-CDx and EVs in D_2O at 3 (middle panel) and 7 days (bottom panel); the yellow symbol represents the assignable peak from C_{60}-**2**. (d) Changes in UV-vis absorption spectra of C_{60}-**2** *via* the exchange reaction between γ-CDx and EVs (bottom panel). (e) Representative image of EVs/C_{60}-**2** morphology. Samples cast on the grid were stained with 0.1% phosphotungstic acid and were observed *via* TEM (acceleration voltage, 80 kV). (f) Conversion of ABDA to endoperoxide *via* oxidation by $^1O_2$. (g) Detection of the generated $^1O_2$ using ABDA. C_{60} derivatives (C_{60}-**1**, C_{60}-**2**, 20 μM) complexed with EVs or liposomes (EVs/C_{60}-**1**, red; Lip/C_{60}-**1**, yellow; EVs/C_{60}-**2**, blue; Lip/C_{60}-**2**, green) were co-incubated with ABDA (12.5 μM) and the resulting dispersion was irradiated at 680–800 nm. The consumption of ABDA was quantified with changes in absorbance at 398.5 nm. Data represents mean ± SD (n = 3).

Table 1 Solution properties of EV loaded with fullerene C_{60} derivatives

	[C_{60}-***X***]^a/mM	D_{hy}^{b}/nm	Average diameter^c/nm	ζ-potential^d/mV
EVs	0		180	−14.0 ± 6
EVs/C_{60}-**1**	0.1		140	−18.7 ± 0.3
EVs/C_{60}-**2**	0.1		170	−25.4 ± 0.9
Lip/C_{60}-**1**	0.1	190 ± 20 (0.24)		+1.46 ± 2
Lip/C_{60}-**2**	0.1	460 ± 16 (0.41)		−5.97 ± 1

^{a} Concentrations of introduced fullerene C_{60} derivatives were determined by absorbance. ^{b} D_{hy} was determined for liposomes *via* DLS measurements performed at 25 °C. ^{c} Average diameter of EVs was calculated *via* NTA. ^{d} ζ-potential was measured using a capillary cell at 25 °C, pH 7.4.

system,[8,9,20] indicating the fullerenes were successfully loaded into EVs whose diffusion constant is larger than γ-CD complex. Moreover, the UV-vis absorption spectra of C_{60}-**2** broadened with time (Fig. 2d). Similar trends were found in the case of C_{60}-**1** (Fig. S1 and S2, ESI†). Here, ultracentrifugation for C_{60}/EVs could remove all the γ-CD (Fig. S3, ESI†), indicating the fullerene derivatives were introduced to EVs *via* not γ-CD complex form but free form. In addition, we prepared fullerene derivatives encapsulated in liposomes (Lip/C_{60}-**1** and Lip/C_{60}-**2**) by exchanging reactions as previously reported (C_{60}, 0.20 mM; EVs, 0.25 mg mL^{-1}; 80 °C). The exchange reaction was completed within 2 h (Fig. S4, ESI†). DLS measurements revealed that the hydrodynamic diameter (D_{hy}) increased from 100 to 190 nm. The time for exchanging reactions for EVs took much longer than that for the liposomal system. As we incubated the mixture of EVs and C_{60}·γ-CD at 40 °C to avoid undesirable denaturing of proteins expressed in EVs, the thermal energy was insufficient to decompose the inclusion complex, which is the dominant driving force for the exchange reaction. NTA measurements revealed that the size distribution of EVs and the number of EVs did not significantly change (Fig. 2a red and blue line), and the spherical morphology of EVs was preserved even after the exchange reaction (Fig. 2e and Fig. S5, ESI†). In addition, there are not significant changes in protein concentration between EVs dispersion and resulting dispersion prepared by exchanging reaction. These results clearly indicate that the loading of C_{60} derivatives can be

 This journal is © The Royal Society of Chemistry 2024

Published on 31 August 2024. Downloaded on 2/13/2026 2:46:06 PM.

achieved without forming undesirable aggregates and precipitates under the current conditions. For these results, 8.0×10^5 molecules of fullerene derivatives were trapped in each EVs.

To demonstrate the photodynamic activity of EVs/C_{60} and Lip/C_{60}, the $^1O_2$-generation capacity was determined by the conversion of 9,10-anthracenediyl-bis(methylene)dimalonic acid (ABDA) to endoperoxide (Fig. 2f).[21] When ABDA was consumed by oxidation by the generated $^1O_2$, the absorbance from anthracene was quenched, as shown in Fig. S5 (ESI†). EVs/C_{60}-**1**, EVs/C_{60}-**2**, Lip/C_{60}-**1**, and Lip/C_{60}-**2** (C_{60}-**1**, C_{60}-**2**; 20 μM) were co-incubated with ABDA (12.5 μM) and irradiated with light (>620 nm). At 60 min of photoirradiation, EVs/C_{60}-**1**, EVs/C_{60}-**2**, Lip/C_{60}-**1**, and Lip/C_{60}-**2** consumed 28%, 8%, 12%, and 0% of ABDA *via* photoirradiation, respectively (Fig. 2g and Fig. S6, ESI†). EVs/C_{60}-**1** exhibited the highest photodynamic activity among these four systems. Moreover, none of systems exhibited precipitation, and the absorption from fullerene derivatives did not decrease during photoirradiation (Fig. S7, ESI†), indicating that these systems were stable with exposure to light. As more polarized fullerenes can be located on the surface where dissolved oxygen can address to achieve energy transfer, C_{60}-**1** systems could convert $^3O_2$ into $^1O_2$ more efficiently than C_{60}-**2** systems. In addition, EV systems showed higher activity than the liposomal system. Consequently, EVs systems are expected to be excellent delivery platforms for fullerene derivatives by manipulating the location in EVs components. To determine quantum yields (Φ) for these systems, we further examined ABDA bleaching test for water soluble photosensitizer, methylene blue (MB; Φ, 0.52;[22] Fig. S8, ESI†). By comparing MB, the Φ of EVs/C_{60}-**1**, EVs/C_{60}-**2**, Lip/C_{60}-**1**, and Lip/C_{60}-**1** were determined to be 0.043, 0.00029, 0.043, and 0.000024, respectively.

Therapeutic efficacy of PDT using EVs incorporating fullerenes *in vitro*

To address the suitability of EV-based delivery systems for fullerenes, we examined the cytotoxicity of EVs toward murine myoblast cells (C2C12) and murine tendon cells as healthy tissue-derived cell lines. After 24 h of incubation, EVs did not induce severe cytotoxicity toward either of these cell lines (Fig. 3a), indicating that current systems have low toxicity and high biocompatibility as drug carriers. We next investigated the photodynamic activity of EVs/C_{60} and Lip/C_{60} toward several cancer cells, including murine colon cancer (Colon26), human cervical cancer (HeLa), and human adenocarcinoma cells (A549). As a control for the experiment, we employed a clinically available photosensitizer based on a water dispersible porphyrin oligomer, PF. Although EVs/C_{60}-**1** and Lip/C_{60}-**1** showed higher photodynamic activity than EVs/C_{60}-**2** or Lip/C_{60}-**2**, cytotoxicity was found even in dark conditions (Fig. S9, ESI†), which can induce side effects. The cytotoxicity may be caused by the cationic character of C_{60}-**1**, which can induce damage to the anionic plasma membrane and mitochondrial membrane.[23] However, neither the EVs/C_{60}-**2** nor Lip/C_{60}-**2** systems showed any apparent cytotoxicity in dark conditions (Fig. 3b and Fig. S10, ESI†). These results suggest that C_{60}-**2**–loading systems are more appropriate as photosensitizers than C_{60}-**1**–loading systems because of their sensitivity to light, which can lessen side effects. Although cytotoxicity under dark conditions decreased, Lip/C_{60}-**2** could not kill these three cancer cell lines even at the highest concentration under light irradiation. Conversely, photoirradiation of cancer cells treated with EVs/C_{60}-**2** enabled induction of cell death in the cell lines. Moreover, the photodynamic activity of EVs/C_{60}-**2** toward Colon26 and A549 higher photodynamic activity than that of the clinically available photosensitizer PF (Table 2). No significant differences in IC_{50} value were present for HeLa cells between PF and EVs/C_{60}-**2** treatments. These results clearly indicate that EV/C_{60}-**2** systems can be widely used as photosensitizers for cancer treatment.

To address their excellent photodynamic activity *in vitro*, we verified the cellular uptake amount of cargo delivered by EVs using 4-chloro-7-nitro-2,1,3-benzoxadiazole (NBD) as a model fluorophore. NBD was also introduced to EVs *via* an exchange reaction as mentioned above.[24] Briefly, NBD hydroxypropyl-β-cyclodextrin (HP-β-CDx) was prepared by HSVM (HP-β-CDx, 15.0 mg; 10 μmol: NBD, 1 mg; 5 μmol). The complex of NBD with HP-β-CDx was co-incubated with EVs (NBD, 0.20 mM; EVs, 0.25 mg mL^{-1}) at 40 °C. As NBD is sensitive to the hydrophobicity of the microenvironment, the exchange process was confirmed by measuring the fluorescence spectra.[25] After 7 days of incubation, the fluorescence from NBD increased (Fig. S11, ESI†), indicating that NBD molecules were translocated to a more hydrophobic environment, such as that on lipid membranes, from the cyclodextrin cavity. This clearly supports that the exchange reaction was successfully achieved with NBD.

To investigate the cellular uptake efficiencies of cargo molecules, EVs/NBD or Lip/NBD were exposed to Colon26, HeLa, and A549 cells. After 24 h of incubation, the cellular uptake amounts of NBD were quantified by measuring the fluorescence of NBD in the lysate of the treated cells. As shown in Fig. 3c, the EV system could deliver three- to fourfold more cargo molecules than liposomal systems to these three cancer cell lines. The excellent deliverability of EVs enabled the enhancement of photodynamic activity *in vitro*, and this feature is attractive for establishing delivery platforms for cancer therapy. We further addressed the cellular uptake mechanism of the EV system by maintaining the cells at 4 °C to inhibit energy-dependent cellular events, including endocytosis.[26] Interestingly, our systems could deliver cargo molecules toward these three cell lines even under endocytosis inhibitory conditions at the same level as the cells actively uptake exogenous interests *via* endocytosis (Fig. 3d). This suggests that our system can be taken up in an endocytosis-independent manner, such as by membrane fusion and direct penetration.[27] The features in the cellular uptake of EVs may affect the efficient accumulation of cargo molecules in cancer cells. We used a confocal laser scanning microscope to investigate the cellular uptake of the current system with a commercially available lipophilic dye, 1,1′-dioctadecyl-3,3,3′,3′-tetramethylindocarbocyanine perchlorate (DiI), To visualize the distribution of liposomes and EVs, Colon26 cells were coincubated with DiI-stained NBD/Lip (DiI-NBD/Lip) or NBD/EVs (DiI-NBD/EVs) for 24 h. As shown in Fig. 3e, fluorescence signals from DiI and NBD were found

Published on 31 August 2024. Downloaded on 2/13/2026 2:46:06 PM.

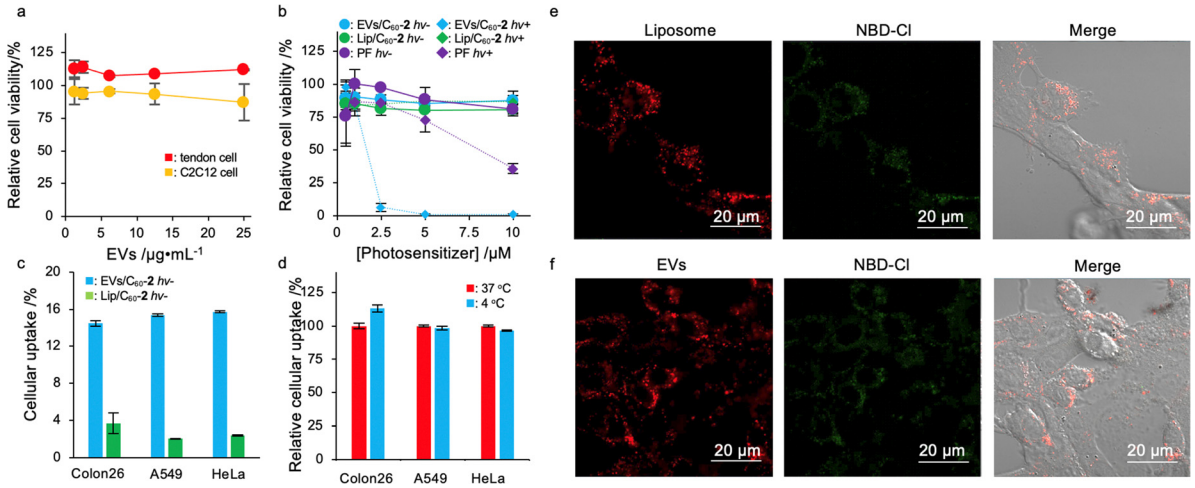

Fig. 3 Photodynamic activity of EVs/C_{60} derivatives *in vitro*. (a) Biocompatibility of EVs with healthy cells. Murine myoblast cells (C2C12, yellow) and murine tendon cells (red) were co-incubated with EVs at varying concentrations for 24 h. Tendon cells were used as the primary culture cells, which were established from C57BL6 mice. Cell viability was estimated *via* WST-8 viability assay. Data represents mean ± SD (n = 3). (b) Photodynamic activity of EVs/C_{60}-**2** toward Colon26 cells. Colon26 cells were exposed to PF (purple), EVs/C_{60}-**2** (blue), or Lip/C_{60}-**2** (green). Treated cells were irradiated with the optimal wavelength (square, dashed line) while the other group was incubated under dark conditions (circle, solid line). After an additional 24 h, cell viability was estimated *via* WST-8 assay. Data represents mean ± SD (n = 3). (c) Cellular uptake of model fluorophore. Colon26, A549, or HeLa cells were co-incubated with EVs/NBD-Cl (pale blue) or Lip/NBD/Cl (pale red) for 24 h ([NBD-Cl], 0.1 mM). The cellular uptake amount was quantified by measuring fluorescence from NBD-Cl, which was obtained from cellular lysates. Data represents mean ± SD (n = 3). (d) Endocytosis inhibition assay for the EV system. Colon26, A549, or HeLa cells were co-incubated with EVs/NBD-Cl at 4 °C (pale blue) or 37 °C (pale red) for 4 h. The ratio of cellular uptake was calculated as the cellular uptake amount at 4 °C per cellular uptake amount at 37 °C. (e) Subcellular distribution of delivered liposomes and cargo molecules. Colon26 cells were exposed to NBD-Cl/Lip for 24 h. After washing with PBS, the sample was observed *via* confocal laser scanning microscopy. (f) Subcellular distribution of delivered EVs and cargo molecules. Colon26 cells were exposed to NBD-Cl/EVs for 24 h. After washing with PBS, the sample was observed *via* confocal laser scanning microscopy.

Table 2 Photodynamic activity *in vitro*

	EVs/C_{60}-**2**/μM	Lip/C_{60}-**2**/μM	PF/μM
Colon26	1.7	10<	8.0
HeLa	0.92	10<	0.77
A549	2.3	10<	8.4

within cells and highly overlapped, indicating that a large part of the delivered cargo molecules remained trapped in liposomes. For DiI-NBD/EVs, both fluorescence signals were also detected within cells as well as in the liposomal system (Fig. 3f); however, the overlap efficiencies between NBD and DiI were lower than those delivered by liposomes, suggesting that the EV system is more efficient than liposomal systems at releasing cargo molecules. This may imply differences in the integrated area of cargo molecules. For liposomes, almost all the hydrophobic compounds should be trapped by the liposomal membrane and the cargo will be highly stabilized, which can strongly bind cargo molecules within liposomal systems. Conversely, EVs not only provide a membrane but also a highly dense polysaccharide layer and membrane proteins for integration, which can easily release interests within cells by interacting with cytosolic biomolecules such as membrane structures and highly concentrated proteins. To address detailed subcellular distribution of cargo molecules delivered by EVs, lysosomes were stained by commercially available lysosome staining reagent, Lysotracker Red. As a result, delivered NBD-Cl were rarely overlapped with Lysotracker Red, indicating that cargo molecules are located in cytosol (Fig. S12, ESI†). The cytosolic delivery is advantageous in inducing oxidative stress to mitochondria and nuclei, which is considered as one of the dominant factors in killing cancer cells in PDT. These facts in deliverability of EVs should enhanced photodynamic activity of fullerene derivatives.

Therapeutic efficacy of PDT using EVs incorporating fullerenes *in vivo*

Finally, we demonstrated photodynamic activity of C_{60} encapsulated by EVs toward tumor xenograft mice. Tumor xenograft mice were established by transplantation of Colon26 cells (1.0×10^5 cells) to the right femur of Balb/c mice (male, 4-week-old, 18 g)[28] and the mice were incubated for 7 days. When the tumor volume was grown up to approximately 20 mm^3, PBS, Lip/C_{60}-**2**, or EVs/C_{60}-**2** (C_{60}, 0.20 mM; 100 μL) were administrated *via* tail vein. At 24 h-post injection, photoirradiation was carried out to the tumor tissue for 1 h (>600 nm, 15 mW) and tumor volume and body weight was measured at each time point (Fig. S13, ESI†). At 14 days post irradiation, photodynamic activity of EVs/C_{60}-**2** were 2.6-fold higher than that of Lip/C_{60}-**2** (Fig. 4a). During the period, no obvious body weight changes were found in all the group (Fig. 4b), indicating all systems can lessen side effects including photoinduced toxicity. These results clearly indicate that EVs systems are effective photosensitizer for PDT.

 This journal is © The Royal Society of Chemistry 2024

Published on 31 August 2024. Downloaded on 2/13/2026 2:46:06 PM.

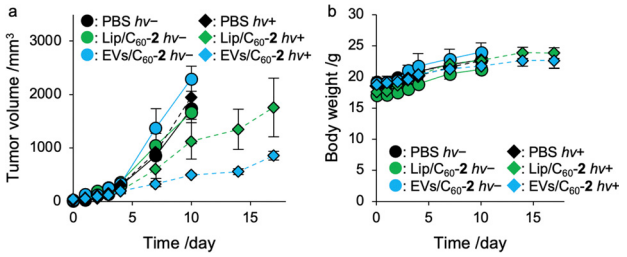

Fig. 4 Photodynamic activity *in vivo*. (a) Tumor growth curve in tumor xenograft mice. Tumor xenograft mice which were established by transplantation of Colon 26 cells were treated with PBS (black), Lip/C_{60}-**2** (green), or EVs/C_{60}-**2** (blue). After 24 h post-injection, the tumor was irradiated with (diamond) or without (circle) light for 1 h. The tumor volume was measured at each time point. (b) Body weight change in tumor xenograft mice.

Conclusion

We developed a hydrophobic compound–loading technique for EVs without using an organic solvent, which can potentially disrupt EV structures. We successfully introduced fullerenes to EVs quantitatively without precipitation by mixing EVs and C_{60}·γ-CD complexes in aqueous media. ^{1}H-NMR spectra showed that the fullerenes were inserted into the EVs by an exchange reaction as indicated by the disappearance of the C_{60}/γ-CD specific peak. The prepared EVs/C_{60} showed an ($^1O_2$)-generating capacity and photodynamic activity comparable or superior with that of Lip/C_{60} prepared using a similar procedure. In addition, the photodynamic activity of EVs/C_{60}-**2** on cancer cells was observed to be superior to that of Lip/C_{60}-**2** and the commercially available photosensitizer PF. Overall, the exchange reaction is a powerful means to introduce hydrophobic compounds to EVs without using harmful organic solvents, and we expect our system to be a photosensitizer that can be applied to PDT.

Author contributions

R. K., N. K., and A. O. mainly performed all the experiments. K. N., K. Y., and D. Y. supported the biological assays. S. M., N. A., A. I., and R. K. designed the systems. N. T. and T. N. conducted animal experiments. N. K., R. K., and A. I. mainly wrote this manuscript. All authors have conducted and approved the final manuscript.

Data availability

No primary research results, software or code have been included and no new data were generated by this paper.

Conflicts of interest

There are no conflicts to declare.

Acknowledgements

This work was supported by the Japan Society for the Promotion of Science, KAKENHI (R. K., JP22K18196). Experiments using transmission electron microscopy were conducted at the Natural Science Center for Basic Research and Development (N-BARD). The author would like to thank Enago (**https://www.enago.jp**) for the English language review.

Notes and references

1 I. K. Herrmann, M. J. A. Wood and G. Fuhrman, *Nat. Nanotechnol.*, 2021, **16**, 748–759.
2 P. E. M. Castilla, L. Tong, C. Huang, A. M. Sofias, G. Pastorin, X. Chen, G. Storm, R. M. Schiffelers and J.-W. Wang, *Adv. Drug Delivery Rev.*, 2021, **175**, 113801.
3 K.-J. Lo, M.-H. Wang, C.-T. Ho and M.-H. Pan, *J. Agri. Food Chem.*, 2024, **72**, 2853–2878.
4 M. Cao, N. Diao, X. Chen, Y. Xiao, C. Guo, D. Chen and X. Zhang, *Mater. Horiz.*, 2023, **10**, 3879–3894.
5 R. Kar, R. Dhar, S. Mukherjee, S. Nag, S. Gorai, N. Mukerjee, D. Mukherjee, R. Vatsa, M. Chandrakanth Jadhav, A. Ghosh, A. Devi, A. Krishnan and N. D. Thorat, *ACS Biomater. Sci. Eng.*, 2023, **9**, 577–594.
6 M. Ruzycka-Ayoush, A. M. Nowicka, A. Kowalczyk, A. Gluchowska, A. Targonska, G. Mosieniak, K. Sobczak, M. Donten and I. P. Grudzinski, *Eur. J. Pharm. Sci.*, 2023, **181**, 106369.
7 S. Kartik Kumar and W. V. Sasidhar, *Mol. Pharm.*, 2023, **20**(8), 3829–3842.
8 R. Kawasaki and A. Ikeda, *ChemBioChem*, 2023, **24**, e202300455.
9 R. Shimada, S. Hino, K. Yamana, R. Kawasaki, T. Konishi and A. Ikeda, *ACS Med. Chem. Lett.*, 2022, **13**(4), 641–647.
10 K. Nishimura, K. Yamana, R. Kawasaki and A. Ikeda, *Org. Biomol. Chem.*, 2023, **21**, 4810–4816.
11 J. Chen, T. Fan, Z. Xie, Q. Zeng, P. Xue, T. Zheng, Y. Chen, X. Luo and H. Zhang, *Biomaterials*, 2020, **237**, 119827.
12 S. Li, F. Yang, Y. Wamng, T. Du and X. Hou, *Chem. Eng. J.*, 2023, **451**, 138621.
13 T. C. Pham, V.-N. Nguyen, Y. Choi, S. Lee and J. Yoon, *Chem. Rev.*, 2021, **121**(21), 13454–13619.
14 J. Zou, L. Li, J. Zhu, X. Li, Z. Yang, W. Huang and X. Chen, *Adv. Mater.*, 2021, **33**, e2103627.
15 E. Öztürk Gündüz, M. E. Gedik, G. Günaydın and E. Okutan, *ChemMedChem*, 2022, **17**, e202100693.
16 A. Akbar, S. Khan, T. Chatterjee and M. Ghosh, *J. Photochem. Photobiol., B*, 2023, **248**, 112796.
17 D. Li, S. Cai, P. Wang, H. Cheng, B. Cheng, Y. Zhang and G. Liu, *Adv. Healthcare Mater.*, 2023, **12**, 230063.
18 C. Lei, Y. Teng, L. He, M. Sayed, J. Mu, F. Xu, X. Zhang, A. Kumar, K. Sundaram, M. K. Sriwastva, L. Zhang, S. Y. Chen, W. Feng, S. Zhang, J. Yan, J. W. Park, M. K. Merchant, X. Zhang and H.-G. Zhang, *iScience*, 2021, **24**, 102511.
19 S. Raimondo, O. Urzì, S. Meraviglia, M. D. Simone, A. M. Corsale, N. R. Ganji, A. P. Piccionello, G. Polito, E. L. Presti, F. Dieli, A. Conigliaro and R. Alessandro, *J. Cell. Mol. Med.*, 2022, **9**, 2105274.

20 A. Ikeda, T. Iizuka, N. Maekubo, R. Aono, J. Kikuchi, M. Akiyama, T. Konishi, T. Ogawa, N. Ishida-Kitagawa, H. Tanabe and K. Shiozaki, *ACS Med. Chem. Lett.*, 2013, **4**(8), 752–756.
21 T. Entradas, S. Waldron and M. Volk, *J. Photochem. Photobiol., B*, 2020, **204**, 111787.
22 D. Gabrielli, E. Belisle, D. Severino, A. J. Kowaltowski and M. S. Baptista, *Photochem. Photobiol.*, 2004, **79**, 227–232.
23 T. Xia, M. Kovochich, M. Liong, J. I. Zink and A. E. Nel, *ASC Nano*, 2008, **2**(1), 85–96.
24 R. Kawasaki, A. Oshige, K. Yamana, H. Hirano, K. Nishimura, Y. Miura, R. Yorioka, Y. Sanada, K. Bando, A. Tabata, K. Yasuhara, Y. Miyazaki, W. Shinoda, T. Nishimura, H. Azuma, T. Takata, Y. Sakurai, H. Tanaka, M. Suzuki, T. Nagasaki and A. Ikeda, *Chem. – Eur. J.*, 2023, **29**, e202302486.
25 Z. Ma, Y. Lin, H. Chen, L. Du and M. Li, *RSC Adv.*, 2016, **6**, 102773.
26 J. J. Rennik, A. P. R. Johnston and R. G. Parton, *Nat. Nanotechnol.*, 2021, **16**, 266–276.
27 N. Kastelowitz and H. Yin, *ChemBioChem*, 2014, **15**, 923–928.
28 R. Kawasaki, R. Ohdake, K. Yamana, T. Eto, K. Sugikawa and A. Ikeda, *J. Mater. Chem. B*, 2021, **9**, 6357–6363.

Published on 31 August 2024. Downloaded on 2/13/2026 2:46:06 PM.

This journal is © The Royal Society of Chemistry 2024